The Natural Ligand for Metalloproteinase-Multifaceted Drug Target

Saranya Shivashankar

B.S.Abdur Rahman Crescent Institute of Science and Technology https://orcid.org/0000-0001-6440-0191

Sangeetha MK (sangeetha@crescent.education)

B.S.Abdur Rahman Crescent Institute of Science and Technology

Research Article

Keywords: Andrographis paniculata, snake venom, phytochemicals, ADAM, batimastat, Autodock.

Posted Date: August 5th, 2021

DOI: https://doi.org/10.21203/rs.3.rs-769330/v1

Version of Record: A version of this preprint was published at Applied Biochemistry and Biotechnology on January 8th, 2022. See the published version at https://doi.org/10.1007/s12010-021-03778-4.

Abstract

Metalloproteinases are a group of proteinases that extensively depend on metals for their biological activity, i.e., digesting proteins. Their role in developmental stages is indispensable. However, the same enzyme is also found to be a crucial mediator of several diseases like cancer, atheroma, arthritis, atherosclerosis, aneurysms, nephritis, tissue ulcers, fibrosis, etc. Exogenous metalloproteinases cause severe pathological effects which may even lead to mortality in humans and other higher animals. The major source of exogenous metalloproteinases is through venomous snake bites, which causes exposure of normal tissue later blood vessels to the proteinases. Though the structure and function of metalloproteinases are highly conserved, the accidental exposure causes severe irreversible damages of the exposed tissues and blood vessels which otherwise is a highly regulated process with the endogenous metalloproteinases. Hence, finding a suitable metalloproteinases inhibitor is of great biological importance in mitigating pathological effects. Batimastat is an approved drug prescribed for cancer which mediates its action by inhibiting metalloproteinases. Batimastat is a synthetic hydroxamate molecule with a simple structure that prompted the search for the existence of similar phytochemicals in plants. Computational analysis revealed interaction of Andrographis paniculata phytochemicals with the M domain of snake venom metalloproteinase active site amino acid residues namely ASN203, ARG293, PHE203, LEU206, LYS199, and ALA122 similar to that of the reference compound batimastat. 14-acetylandrographolide, 14-deoxy-11,12 didehydroandrographolide, Andrograpanin, Isoandrographolide, and 14-deoxy-11-oxoandrographolide found to show maximum effectiveness against the metalloproteinase. Results of the current study show a possibility of developing potent drug targeting metalloproteinases from plants source.

1. Introduction

Metalloproteinase are ECM (extracellular matrix) remodeling endopeptidases that can degrade the ECM component. Extracellular matrix degradation is a significant feature for cellular development, morphogenesis, repair, and remodeling of tissues, ever since it is associated with embryonic development and angiogenesis (1). Apart from supporting role for tissues and organs, ECM also participates in the cell cycle regulation and motility, apoptosis, growth factor distribution, and signal integration into the cells. ECM is made of hundreds of molecules including metalloproteinase (2). Metalloproteinase contains zinc and calcium that timely degrade, remodel the ECM proteins. They also involve in various physiological processes regulated by cytokines, hormones, and growth factors (3). Exogenous metalloproteinase cause extreme pathological effects which may even lead serious adverse reaction and mortality in humans and other higher animals. Exogenous metalloproteinases major source of is through venomous snake bites. Snake venom metalloproteinase (SVMP), a major constituent of the viper family - especially Russell's viper (D. russelli), is peaking up to 24% of the whole venom (4). SVMP targets capillaries and blood vessels as it selectively breaks the basement membrane's significant bonds thereby affecting the cell membrane and endothelium interaction resulting in hemorrhage followed by cellular shock, inflammation, hypovolemia, hypotension, necrosis of tissue, and impaired regeneration of muscle tissue (5).

According to WHO, India is home to nearly twenty-four medically important snake species. Of which Russell's viper is classified under Category 1 (Highest medical importance) "highly venomous snakes that are common or widespread and cause numerous snakebites, resulting in high levels of morbidity, disability or mortality" (6). In India, Russell's viper is one of the 'Big four' snakes causing the maximum number of deaths due to snakebite (7). Snakebite statistics from 2000-2019 reveal Russell's viper is mainly responsible for bite constituting43%, followed by 21% unknown species, 18% Krait, 12% cobra (8).

Hence SVMP is seen as a promising target for treatment against adverse effects of snake venom. This would reduce the mortality rate among snake-bitten patients. In traditional medicine practice, the decoction of various plant parts are been used in several parts of Asia, Africa, Central, and South America for treating snake envenomation (9). *Andrographis paniculata* is a remarkable plant used for treating various human ailments namely anti-cancer, antidiabetic, antibacterial, antimalarial, antiviral, cardiovascular, and hepatic protection (10) including venom neutralization (11). Previously, we reported that the trimethoprim resistant *Staphylococcus aureus* dihydrofolate reductase inhibition by *A.paniculata* phytochemicals (12). The traditional use of *A. paniculata* for venom neutralization is equally supported by modern scientific studies. The current study addresses the natural SVMP ligand in *A. paniculata* phytochemicals using the *in-silico* method.

2. Material And Methods

2.1 *A.paniculata* phytochemicals and target protein selection

Structures of *A.paniculata* phytochemicals and reference compound batimastat, a known inhibitor of metalloproteinase, collected from PubChem database (https://pubchem.ncbi.nlm.nih.gov/). List of ligands for the present study were 14-acetylandrgrapholide (CID_73353957), 14-deoxy-11,12didehydroandrographolide (CID_5708351), 14-deoxy-11-oxoandrographolide (CID_101593061), Andrograpanin (CID_11666871), Andrographidine A (CID_13963762), Andrographidine C (CID_5318484), Andrographidine E (CID_13963769), Andrograhin (CID_5318506), Andrographiside (CID_44593583), Andrographolide (CID_5318517), Andrographoside (CID_6439612), Andropanolide (CID_7067324), Andropanoside (CID_44575270), Bisandrographolide (CID_12000062), Chlorogenic acid (CID_1794427), Deoxyandrographolide (CID_21679042), Isoandrographolide (CID_101563021), Myristic acid (CID_11005), Neoandrographolide (CID_9848024), Paniculide A (CID_11821485), Paniculide B (CID_101289823), Paniculide C (CID_101289824) and Batimastat (CID_5362422). Three-dimensional structure of ligands are presented in **Fig1**

A 2.91 Å resolution of SVMP crystal structure was downloaded from the Protein Data Bank (PDB), which is managed by the Research Collaboratory for Structural Bioinformatics (RCSB) (https://www.rcsb.org/), as a PDB file (PDB ID: 2E3X). The three-dimensional structure of the metalloproteinase is presented in **Fig2**

2.2 Target protein binding site prediction

The binding site/pocket of SVMP was identified using metaPocket 2.0, which is a meta server for identifying the specific sites of peptides and proteins (13).

2.3 Molecular docking analysis

The binding efficiency of *A. paniculata* phytochemicals with SVMP active site was determined using Autodock 4, an *in-silico* method. Water molecules were removed, followed by the addition of polar H-bonds and Kollman charges to the SVMP (target protein). Then the number of torsions was set to the ligand. Both the target protein and ligand were saved in pdbqt file format. For a ligand to bind at the target protein's active site, a grid map was assigned with x, y, z points. Docking was performed using the Lamarckian genetic algorithm. Binding energy, binding residues, inhibition constant analyzed and produced as docking output (14).

2.4 Visualization of protein-ligand interaction

A.paniculata phytochemicals and batimastat docked complex with SVMP were visualized and analyzed using BIOVIA Discovery Studio Visualizer (15).

2.5 Molecular dynamic simulation

The protein-ligand complex flexibility was analyzed using the CAB FLEX 2.0 server. Each amino acid residue fluctuation of the best hit was elucidated based on the RMSF (Root Mean Square Fluctuation) value to analyze the conformational stability of the complex (16).

2.6 Drug-likeness screening and evaluation of ligands

In-silico analysis of pharmacological and drug-likeliness of phytochemicals screened and evaluated using SWISSADME tool (http://www.swissadme.ch/) web tool developed by Daina et al. (17).

2.7 Ligand-based virtual screening

Ligand-based virtual screening was performed for three phytochemicals to find similar analogs from FDA-approved drugs using SwissSimilarity (http://www.swisssimilarity.ch/), an online tool used to identify similar small molecules (18).

2.8 Target prediction

The ligand’s most possible macromolecular targets of *Homo sapiens* were predicted using SwissTargetPrediction (19). Cytoscape software (3.8.2 version) was used to create a phytochemical – target illustration network.

3. Results And Discussion

Globally, snakes are the most dreaded venomous animals since they induce morbidity and mortality greatly. Snakebite envenomation induces local tissue damage including myonecrosis

and inflammation. Pathogenesis induced by snakebite is multifactorial and complex. Many studies reported the association of clinical symptoms with the biochemical variation of venom composition (20). Snake venom has evolved into a wide range of proteins and peptides that induce neurotoxic, hemotoxic, cytotoxic, inflammatory effects, etc. If not treated envenomation results in severe morbidity and even death. The main protein classes in snake venom causing a severe pathological effect in victims are three-finger toxins (3FTXs), phospholipase A2 (PLA A2), snake venom serine protease (SVSP), and snake venom metalloproteinase (SVMP) (21). Previously we reported the interaction of *A.paniculata* phytochemicals with PLA A2 of Russell's viper. Phytochemicals had a great affinity towards the residues responsible for the myotoxic and enzymatic activity of PLA A2 (22).

Next to PLA A2, the predominant SVMP becomes the potent target for small pharmaceutical biomolecules. Apart from the hemorrhagic activity of snake venom metalloproteinase other activities namely fibro(ogen)olytic, prothrombin activation, activation of blood coagulation factor X, apoptosis, inhibition of platelet aggregation, pro-inflammatory and blood serine proteinase inhibitor inactivation are also attributed to SVMPs (23). All these factors have envisioned SVMP as a potential target.

SVMP (PDB ID: 2E3X) selected for the study represents class P-IIId, a heterotrimeric class of SVMP, which has MDC (M - metalloproteinase, D - Disintegrin-like, C - Cysteine-rich) domain along with snaclec domain. It is made up of a heavy chain and two light chains namely LA and LB. Cys133, present in the C-terminal of the light chain, bonds (disulfide bond) with Cys389 present in the heavy chain's hyper variable region (HVR) (24). Zinc and calcium are involved in the catalytic activity and structural stabilization of SVMP respectively (25). Russell's viper metalloproteinase is a strong activator of the blood coagulating factor X (FX) (26). During the physiological coagulation, FX is activated upon R194-I195 bond cleavage by the factors IXa or VIIa resulting in the removal of the 52 residues at the N-terminal of the FX heavy chain which is heavily glycosylated. This results in the formation of a catalytic triad (the active site in this case) of the serine proteinase domain. Thus, the activated FX (FXa), in turn, facilitates the conversion of prothrombin to thrombin which eventually forms a hemostatic plug (27-29). Hence, SVMP is seen as one of the crucial proteins mediating the venomous activity of snake venom.

In cellular processes, the interaction of the protein with other molecules is needed for performing their biological function. Hence knowledge of interacting/functional sites would help us to develop inhibitors for receptor proteins. Therefore, the primary prerequisite step for protein-ligand docking studies is the identification of ligand binding sites Here the binding sites of SVMP are predicted using the metal pocket tool.

MetaPocket analyzes and combines the results obtained from eight predictor tools namely POCASA, LIGSITECS (LCS), Fpocket (FPK), GHECOM (GHE), Q-SiteFinder, ConCavity (CON), SURFNET, and PASS (PAS) to improve the prediction success rate. Metapocket combines' z-score of all 8 predicted autonomous tools which run simultaneously to produce a total z-score. Based on spatial similarity the pocket sites are determined and finally, all the clusters are arranged based on the total z-score as predicted by metapocket. The results are presented in the form of a table highlighting the functional residues which are found in the vicinity of the pocket sites (13). The results are summarized in Table 1, which shows the binding site at the third pocket (C3), with x, y, and z grid points 45.169, 39.898, and -4.220 of the pocket and its total z-score 1.72. Pockets that are ranked first were used for further molecular docking study.

Autodock 4.2 was used to study the binding affinity of various ligands towards SVMP at the molecular level. A two-dimensional structure representing the interaction of *A.paniculata* phytochemicals and batimastat with SVMP is presented in Fig3. Binding energy, inhibition constant, interaction, and interacting amino acids are tabulated in Table 2.

Binding energy is better defined as the aggregate of the torsional free energy and the intermolecular energy of the compounds. In simple terms, the energy released during bond formation or the protein-ligand interaction can be defined as binding energy. However, for any favorable reaction to occur the free energy should be negative. The lower the binding energy, the greater is the protein-ligand binding. The binding energy of 14-acetylandrographolide with

SVMP is higher than -9.32kCal/mol whereas the least binding phytochemical is bisandrographolide with -4.09kCal/mol.

Inhibition constant is the required concentration of inhibitor to produce half-maximum inhibition. Autodock calculates *Ki* as follows:

$$Ki = \exp(\Delta G \times 1000) / Rcal \times TK)$$

Where ΔG is the docking energy,

Rcal is 1.987

TK is 298.15

Docking energy is the summation of the ligand's internal energy and the intermolecular energy (30).

Surprisingly, seven phytochemicals of *A.paniculata* showed higher binding energy than the known SVMP inhibitor batimastat. 14-acetylandrographolide, 14-deoxy-11,12didehydroandrographolide, andrograpanin, Isoandrographolide 14-deoxyandrographolide, Andropanolide, and Andrographolide are the seven phytochemicals of *A.paniculata*. In the present study, all the *A. paniculata* phytochemicals were found to interact with the M domain of the SVMP heavy chain. Phytochemicals form a non-covalent bond with SVMP residues namely GLU14, ILE57, ARG85, MET90, LYS93, SER94, HIS95, ASP96, MET119, CYS120, GLN121, ALA122, LYS197, PRO198, LYS199, CYS200, PHE202, ASN203, PRO204, PRO205, LEU206, ASP209, ARG275, ASP276, ASP279, ARG293, ASP294, GLN295, LEU296, TYR311, ASN312, GLY313, ASP314, ASP398, and PRO399. Non-covalent interactions have a pivotal role in assessing the function, structure, and dynamics of the biomolecules. They are reversible and have favorable energy at room temperature. Non-covalent interactions are strong, sufficient to bind molecules together as well as weak enough to assemble and disassemble without the usage of much energy (31). Batimastat a known inhibitor of SVMP (32) formed a conventional hydrogen bond with only two amino acid residues PHE202 and ASN203. Whereas the phytochemicals of *A. paniculata* found to form conventional hydrogen bonds besides PHE202 and ASN203, are ARG293 and ASP294 of calcium-binding region owing to higher binding efficiency. Catalytic calcium-binding site residues interacting with the ligands are presented in **Fig4**. Eighteen out of twenty-two phytochemicals formed a conventional hydrogen bond with PHE202, ASN203, ARG293, and ASP294 amino acids except for Deoxyandrographolide, andrographidine C, andrographidine E, and Bisandrographolide. Hydrogen bonding between a druggable ligand and a protein receptor is strong and has high specificity (33). Three different effects rise from hydrogen bonds in ligand binding namely: (i) positioning of ligand by a binding partner, occasionally related to molecule conformational distortion, (ii) substrates recognition, and (iii) ligand affinity. However, they affect the molecule's physiochemical properties (34).

Protein structural flexibility plays a key role in biological function. Metalloproteinase and its complex flexibility with phytochemicals were simulated using Cab Flex 2.0, an online server. Structural simulation results show that the RMSF of amino acids was comparatively low for metalloproteinase-ligand complex than the metalloproteinase unbound state. 14-deoxy-11,12didehydroandrographolide, Andrograpanin, and 14-deoxy-11-oxoandrographolide had high fluctuation when compared with 14-acetylandrographolide, Isoandrographolide, Andropanolide, andrographolide and batimastat. Molecular dynamic simulations of the metalloproteinase-ligand complex are presented in **Fig5**. The change in the amino acids fluctuation at the active site metalloproteinase indicates binding of phytochemicals, which ultimately enhance the rigidity of amino acids at the protein active site.

SwissADME a web tool predicts ADME parameters and calculates physiochemical descriptors along with pharmacokinetics properties, drug-likeness, and medicinal chemistry of small molecules. In our current study, ligands were evaluated for drug-likeness properties. Results were presented as BOILED-Egg model, a graphical representation. The graphical interface of

BOILED-Egg can predict HIA (passive human gastrointestinal absorption), BBB (Blood-brain barrier) permeation by calculating lipophilicity (WLOGP) versus polarity (TPSA) (17). In our current study, fourteen phytochemicals showed HIA property and seven phytochemicals showed BBB permeation property. The BIOLED-Egg model for *A.paniculata* phytochemicals was shown in **Fig6**.

Structurally unrelated drugs are actively transported (efflux) out of the cell against the concentration gradient by P-glycoprotein (P-gp), membrane-bound transporter) resulting in intracellular concentration reduction, in-turn it affects the drug's oral bioavailability (35). BOILED-Egg model additionally indicated that among twenty-two phytochemicals, fifteen would function as P-gp + (P-gp substrate). The Drug-likeness property of *A.paniculata* phytochemicals is shown in Table 3. 14-acetylandrographolide and Andrograpanin shows P-gp+ and HIA property whereas 14-deoxy-11,12didehydroandrographolide show BBB permeation along with P-gp+ and HIA properties. The results shows the potential use of *A.paniculata* phytochemicals as drug, and the results also suggest ADME parameters guided structural alterations can be made to make versatile drug.

Ligand-based virtual screening (LBVS) done using SwissSimilarity to find similar analogs from FDA-approved drugs for phytochemicals LBVS works based on the hypothesis “Similar molecules are prone to exhibit similar biological activity”. It relies on molecular similarity quantification (36). Phytochemicals were analogous to drugs having antibiotic, anti-inflammatory, antihypertensive, antihypotensive, anti-arrhythmic, anticancer, antidiabetic, antilipidemic, anti-viral, anti-retroviral, anti-malarial, anti-fungal activity with similarity score ranging from 0.002 to 0.887. Ouabain, an anti-arrhythmic drug showed a high similarity score with Andropanoside. Eplerenone, an anti-hypertensive drug analogous to Paniculide A with a high similarity score of 0.513. A histogram presenting the phytochemical similarity score against the FDA approved drug is represented as **Fig7**. However, screening for 14-deoxy-11,12 didehydroandrographolide did not show any similar analogs. SwissSimilarity results with analogs score tabulated as Table 4.

Putative targets of *A.paniculata* phytochemicals were identified through SwissTargetPrediction, a web tool used to find the possible target for small molecules (37). In our current study, we found each phytochemicals would interact and target multiple proteins. This might be the polypharmacology effect of phytochemicals. The phytochemicals which targeted different classes of metalloproteinase were selected and a phytochemical-target illustration network was created using Cytoscape, a software used for visualizing network and integration biomolecular interaction (38). The phytochemical-target network results are presented in **Fig8**.

4. Conclusion

Our current study indicated the strong interaction of *A.paniculata* phytochemicals with the metalloproteinase catalytic M domain. Ligand-based virtual screening showed that phytochemicals were analogs to FDA-approved drugs having antibacterial, anti-inflammatory, anticancer, antidiabetic, antilipidemic, antifungal, antimalarial, and antiviral activity. ADME analysis showed that phytochemicals have a good bioavailability score and can be a potential drug candidate. Target prediction identification revealed that phytochemicals would have multiple protein targets which indicate the polypharmacology effect. Molecular dynamic simulation exhibited binding of *A.paniculata* phytochemicals with metalloproteinase that influences the biological activity. In conclusion, the photochemical of *A.paniculata* was found to be a potent drug targeting metalloproteinase thereby suggesting its use as a drug to neutralize exogenous metalloproteinase in case of snakebite and endogenous metalloproteinase in case of cancer.

Declarations

Funding

Authors thank School of Life Sciences, B.S.Abdur Rahman Crescent Institute of Science and Technology for providing fellowship and research facilities.

Conflicts of interest/Competing interests

The authors declare that they have no known competing financial interests or personal relationships that could have appeared to influence the work reported in this paper.

Availability of data and material

Data and materials available on request

Code availability

Online tools like metaPocket, SwissSimilarity, Swisstargetprediction and Cab Flex 2.0 and Free software Autodock4, Biovia Discovery Studio visualizer 2016 and Cytocape 3.8.2 were used.

Authors' contributions

M.K. Sangeetha – Credits for CONCEPTUALIZATION, SUPERVISION, PROJECT ADMINISTRATION.

Saranya Shivashankar - Credits for WRITING – ORIGINAL DRAFT; WRITING – REVIEW & EDITING, FORMAL ANALYSIS, DATA CURATION, VALIDATION.

ETHICS APPROVAL

Not applicable

CONSENT TO PARTICIPATE

Not applicable

CONSENT FOR PUBLICATION

Not applicable

References

1. Cabral-Pacheco, G.A., Garza-Veloz, I., Castruita-De la Rosa, C., Ramirez-Acuna, J.M., Perez-Romero, B.A., Guerrero-Rodriguez, J.F., Martinez-Avila, N. & Martinez-Fierro, M.L. (2020) The Roles of Matrix Metalloproteinases and Their Inhibitors in Human Diseases Int. J. Mol. Sci. 21(24), 9739.

https://doi.org/10.3390/ijms21249739

2. Cui, N., Hu, M., and Khalil, R.A. (2017) Biochemical and Biological Attributes of Matrix Metalloproteinases. Prog. Mol. Bio. Transl. Sci. 147, 1-53.

https://doi.org/10.1016/bs.pmbts.2017.02.005

3. Kapoor, C., Vaidya, S., Wadhwan, V., Hitesh., Kaur, G. and Pathak, A. (2016) Seesaw of matrix metalloproteinases (MMPs). J. Cancer Res. Ther. 12, 28-35.

http://doi.org/10.4103/0973-1482.157337

4. Kalita, B., Patra, A. and Mukherjee, A.K. (2017) Unravelling the proteome composition and immuno-profiling of western India Russell's viper venom for in-depth understanding of its pharmacological properties, clinical manifestations, and effective antivenom treatment. J. Proteome. Res. 16(2), 582-589.

https://doi.org/10.1021/acs.jproteome.6b00693

5. Chinnasamy, S., Chinnasamy, S., Nagamani, S., and Muthusamy, K. (2014) Identification of potent inhibitors against venom metalloproteinase (SVMP) using molecular docking and molecular dynamics studies. J. Biomol. Struct. Dyn. 1516-1527.

https://doi.org/10.1080/07391102.2014.963146

6. WHO, Venomous snakes distribution.

http://apps.who.int/bloodproducts/snakeantivenoms/database/

7. Upansani, M.S., Upansani, S.V., Beldar, V.G. and Gujarathi, P.P. (2017) Infrequent use of medicinal plants from India in snakebite treatment. Integr. Med. Res. 7(1), 9-26.

https://doi.org/10.1016/j.imr.2017.10.003

8. Suraweera, W., Warrell, D., Romolus, W., Menon, G., Rodrigues, R., Fu, S.H., Begum, R., Sati, P., Piyasena, K., Bhatia, M., Brown, P., and Jha P. (2020) Trends in snake bite deaths in India from 2000 to 2019 in a nationally representative mortality study. eLife.

https://doi.org/10.7554/eLife.54076

9. Pan, S.Y., Zhou, S.F., Gao,S.H., Yu, Z.L., Zhang, S.F., Tang, M.K., Sun, J.N., Ma, Y.F., Han, Y.F., Fong, W.F. and Ko, K.M. (2013) New perspective on how to discover drugs from herbal medicines: CAM's outstanding contribution to modern therapeutics. Evid. Based Complement Alternat. Med. 627375.

https://doi.org/10.1155/2013/627375

10. Dai, Y., Chen, Shao-Ru., Chai, L., Zhao, J., Wang, Y. and Wang, Y. (2019) Overview of pharmacological activities of *Andrographis paniculata* and its major compound andrographolide. Crit. Rev. Sci. Nutr. 59(sup1), S17-S29.

https://doi.org/10.1080/10408398.2018.1501657

11. Janardhan, B., Shrikanth, V.M., Dhanjaya, B.L. and More, S.S. (2015). Antisnake venom property of medicinal plants. Int. J. Pharm. Sci. 7(1), 21-26.

https://innovareacademics.in/journals/index.php/ijpps/article/view/3910

12. Saranya, S. and Sangeetha, M.K. (2021) Identification of Biosimilar for Trimethoprim - *Andrographis paniculata* Phytochemicals Inhibits Dihydrofolate Reductase (DHFR). Biointerface Res. Appl. Chem. 11(6), 14142-14154.

https://doi.org/10.33263/BRIAC116.1414214154

13. Huang, B. (2009) MetaPocket: A meta approach to improve protein ligand binding site prediction. OMICS. 13(4), 325-330.

https://doi.org/10.1089/omi.2009.0045

14. Morris, M.G.,Goodshell, D.S., Halliday R.S., Huey, R., Hart, W.E., Belew, K.R. and Olson, J.A. (1999) Automated Docking using a Lamarkian genetic algorithm and Empirical binding free energy function. J. Comput. Chem. 19, 1639-1662.

https://doi.org/10.1002/(SICI)1096-987X(19981115)19:14%3C1639::AID-JCC10%3E3.0.CO;2-B

15. Biovia, Dassault Systems, Biovia discovery studio visualizer, v17.2.0.16849, San Diego, Dassault Systems, © 2016.
16. Daina, A., Michielin, O., and Zoete, V. (2017) SwissADME: a free web tool to evaluate pharmacokinetics, drug-likeness and medicinal chemistry friendliness of small molecules. Sci. Rep. 7.

https://doi.org/10.1038/srep42717

17. Zoete, V., Diana, A., Bovigny, C., and Michielin, O. (2016) SwissSimilarity: A web tool for low to ultra high throughput ligand-based virtual screening. J. Chem. Inf. Model. 56(8), 1399-1404.

https://doi.org/10.1021/acs.jcim.6b00174

18. Diana, A., Michielin, O., and Zoete, V. (2019). SwissTargetPrediction: updated data and new features for efficient prediction of protein targets of small molecules", Nucleic acids Res. 47(W1), W357-W364.

https://doi.org/10.1093/nar/gkz382

19. Kuriata, A., Gierut, A.M., Oleniecki, T., Ciemny, M.P., Kolinski, A., Kurcinski, M. and Kmiecik, S. (2018). CABS-flex 2.0: a web server for fast simulations of flexibility of protein structures. Nucleic Acids Res. 46(W1), W338-W343.

https://doi.org/10.1093/nar/gky356

20. Fatima, L. and Fatah, C. (2014) Pathophysiological and pharmacological effects of snake venom. J. Clinical Toxicol. 4, 1-9.

https://doi.org/10.4172/2161-0495.1000190

21. Ferraz, C.R., Arrahman, A., Xie, C., Casewell, N.R., Lewis, R.J., Kool, J. and Cardoso, C. (2019) Multifunctional toxins in snake venoms and therapeutic implications: from pain to hemorrhage and necrosis. Front. Ecol. Evol. 7(218).

https://doi.org/10.3389/fevo.2019.00218

22. Saranya, S., Aswini, M. and Sangeetha, M.K. (2019) Molecular interaction of phytochemicals with snake venom: Phytochemicals of *Andrographis paniculata* inhibits phospholipase A2 of Russell's viper (Daboia russelli). Biocatal. Agric. Biotechnol. 18.

https://doi.org/10.1016/j.bcab.2019.101058

23. Markland, F.S Jr. and Swenson, S. (2013) Snake venom metalloproteinase. Toxicon. 62, 3-18.

https://doi.org/10.1016/j.toxicon.2012.09.004

24. Takeda, S., Takeya, H. and Iwanaga, S. (2012) Snake venom metalloproteinase: structure, function and relevance to the mammalian ADAM/ADAMTS family proteins. Biochem. Biophys. Acta. 1824(1), 164-76.

https://doi.org/10.1016/j.bbapap.2011.04.009

25. Fox, J.W. and Serrano, S.M. (2005). Structural consideration of the snake venom metalloproteinase, key members of the M12 reprolysin family of metalloproteinase. Toxicon. 45(8), 969-85.

https://doi.org/10.1016/j.toxicon.2005.02.012

26. Takeda, S., Igarashi, T. and Mori, H. (2007) Crystal structure of RVV-X: an example of evolutionary gain of specificity by ADAM proteinases. FEBS Lett. 581(30), 5859-64.

https://doi.org/10.1016/j.febslet.2007.11.062

27. Takeya, H., Nishida, S., Miyata, T., Kawada, S., Saisaka, Y., Morita, T. and Iwanaga, S. (1992) Coagulation factor X activating enzyme from Russell's viper venom (RVV-X). A novel metalloproteinase with Disintegrin (platelet aggregation inhibitor)-like and C-type lectin-like domains. J. Biol. Chem. 267(20), 14109-17.

https://doi.org/10.1016/S0021-9258(19)49685-3

28. Takeda, S. (2010) Structural aspects of the factor X activator RVV-X from Russell's viper venom, In: Kini,R., Clemetson, K., Markland, F., McLane, M., Morita T.(eds) Toxins and Hemostatasis. Springer, Dordrecht.

https://doi.org/10.1007/978-90-481-9295-3_27

29. Gowda, D.C., Jackson, C.M., Hensley, P. and Davidson, E.A. (1994) Factor X-activating glycoprotein of Russell's viper venom. Polypeptide composition and characterization of the carbohydrate moieties. Biol. Chem. 269(14), 10644-50.

https://doi.org/10.1016/S0021-9258(17)34108-X

30. Iman, M., Saadabadi, A. and Davood, A. (2015). Molecular docking analysis and moleuclr dynamic stimulation study of ameltolide analogous as a sodium channel blocker. Turkish J. Chem. 30, 306-316.

https://doi.org/10.3906/KIM-1402-37

31. Rezac, J. and Hobza, P. (2016) Benchmark calculations of interaction energies in noncolvalent complexes and their applications. Chem. Rev. 116(9), 503-71.

https://doi.org/10.1021/acs.chemrev.5b00526

32. Villalta-Romero, F., Gortat, A., Herrera, A.E., Arguedas, R., Quesada, J., Lopes de Melo, R., Calvete, J.J., Montero, M., Murillo, R., Rucavado, A., Gutierrez, JM. And Perez-Paya, E. (2012) Identification of new snake venom metalloproteinase inhibitor using compound screening and rational peptide design. ACS Med. Chem. Lett. 3(7), 540-543.

https://dx.doi.org/10.1021%2Fml300068r

33. Zhou, P., Huang, J. and Tian, F. (2012) Specific noncovalent interactions at protein-ligand interface: implications for rational drug design. Curr. Med. Chem. 19(2), 226-38.

https://doi.org/10.2174/092986712803414150

34. Kubinyi, H. (2001) Hydrogen bonding, the last mystery in drug discovery?", In Pharmacokinetic optimization in Drug Research: Testa, B., van de Waterbeemd., Folkers, G., R.Eds:Wiley-VCH:Weinheim, 513-524.

https://doi.org/10.1002/9783906390437.ch28

35. Constantinides, P.P., and Wasan, K.M. (2007) Lipid formulation strategies for enhancing intestinal transport and absorption of P-glycoprotein (P-gp) substrate drugs: in vitro/in vivo case studies. J. Pharm. Sci. 96(2), 235-48.

https://doi.org/10.1002/jps.20780

36. Maggiora, G., Vogt, M., Stumple, D., and Bajorath, Jurgen. (2014) Molecular similarity in medicinal chemistry. J. Med. Chem. 57(8), 3186-204.

https://doi.org/10.1021/jm401411z

37. Gfeller, D., Michielin, O. and Zoete, V. (2013). Shaping the interaction landscape of bioactive molecules. Bioinform. 29(23), 3073-3079.

https://doi.org/10.1093/bioinformatics/btt540

38. Shannon, P., Markiel, A., Ozier, O., Baliga, N.S., Wang, J.T., Ramage, D., Schwikowski, B. and Ideker, T. (2003) Cytoscape: a software environment for integrated models of biomolecular interaction networks. Genome Res. 13(11), 2498-504.

https://doi.org/10.1101/gr.1239303

Tables

Due to technical limitations, table 1-4 is only available as a download in the Supplemental Files section.

Figures

Fig1

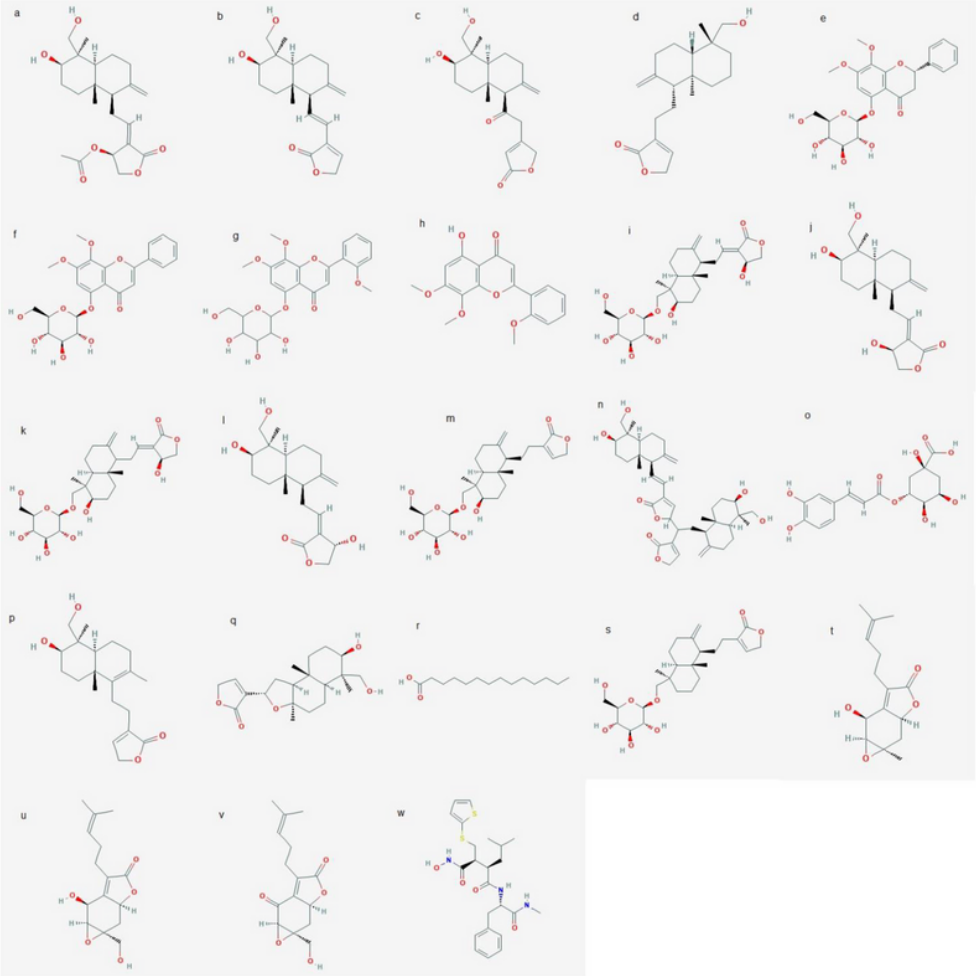

Figure 1

Three-dimensional structure of ligands Legend: a. 14-acetylandrographolide, b. 14-deoxy-11,12didehydroandrographolide, c. 14-deoxy-11-oxoandrographolide, d. Andrograpanin, e. Andrographidine A, f. Andrographidine C, g. Andrographidine E, h. Andrographin, i. Andrographiside, j. Andrographolide, k. Andrographoside, l. Andropanolide, m. Andropanoside, n. Bisandrographolide, o. Chlorogenic acid, p. Deoxyandrographolide, q. Isoandrographolide, r. Myristic acid, s. Neoandrographolide, t. Paniculide A, u. Paniculide B, v. Paniculide C, w. Batimastat

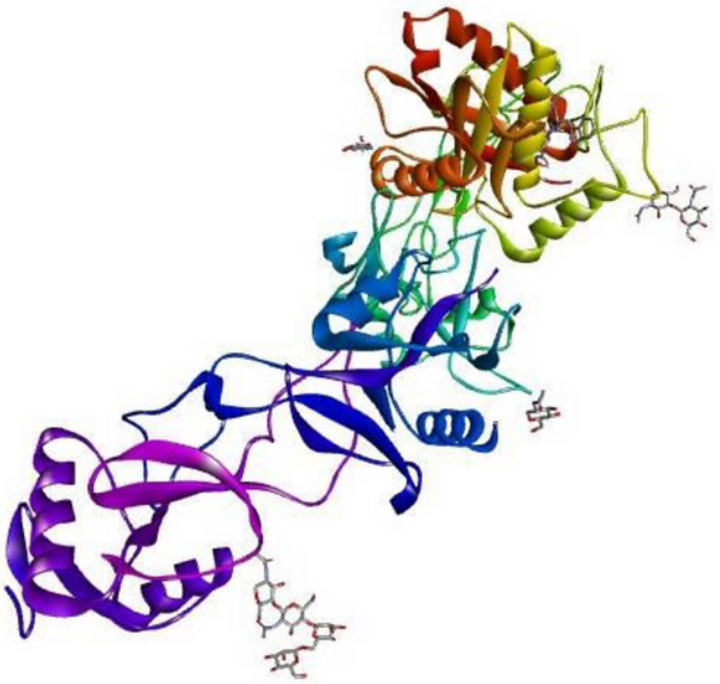

Figure 2

The three-dimensional structure of the metalloproteinase.

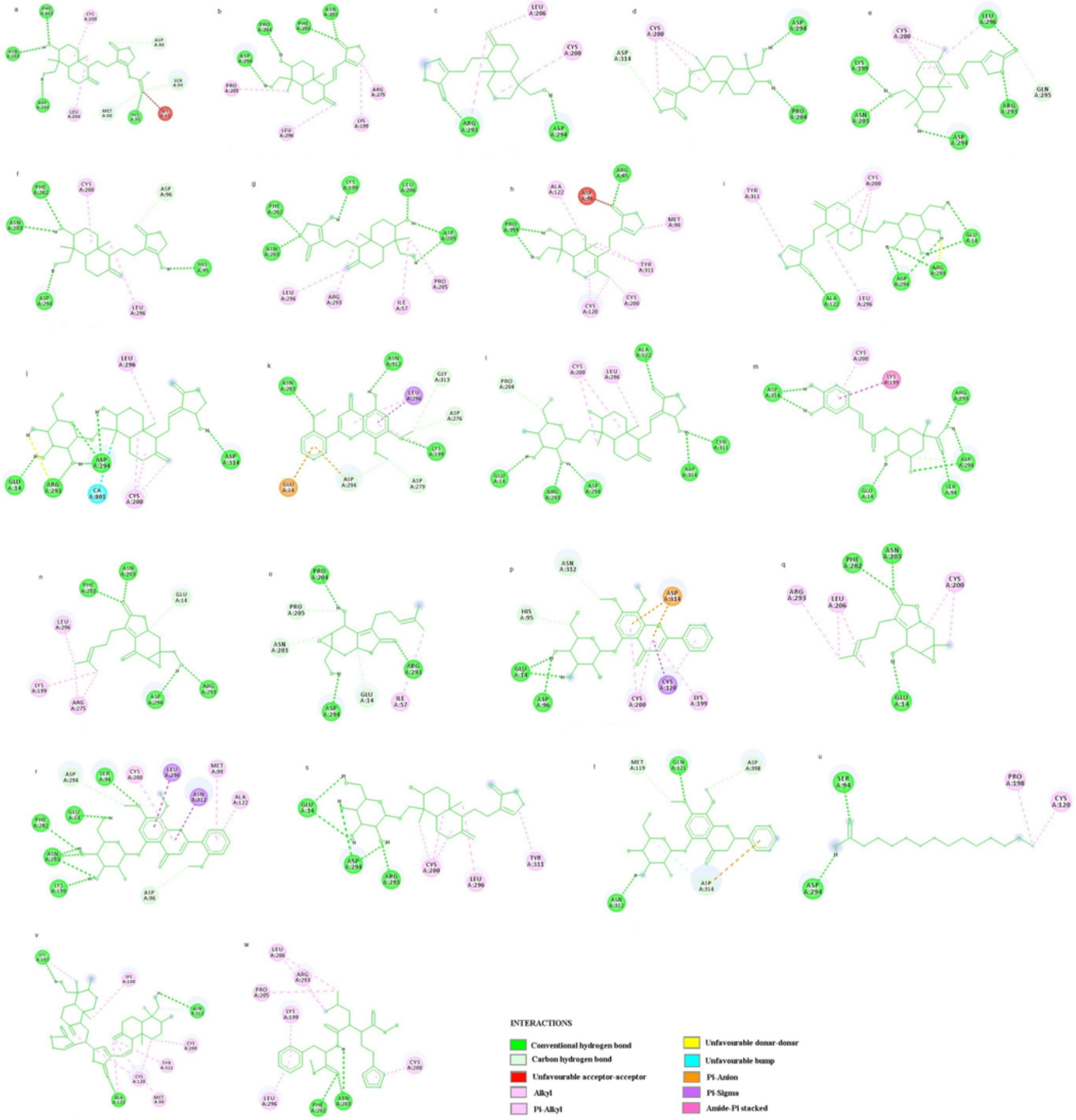

Figure 3

A two-dimensional structure representing the interaction of A.paniculata phytochemicals and batimastat with SVMP Legend: Molecular docking analysis of SVMP with ligands a. 14-acetylandrographolide, b. 14-deoxy-11,12didehydroandrographolide, c. Andrograpanin, d. Isoandrographolide, e. 14-deoxy-11-oxoandrographolide, f. Andropanolide, g. Andrographolide, h. Deoxyandrographolide, i. Neoandrographolide, j. Andrographiside, k. Andrographin, l. Andrographoside, m. Chlorogenic acid, n.

Paniculide C, o. Paniculide B, p. Andrographidine C, q. Paniculide A, r. Andrographidine E. s. Andropanoside, t. Andrographidine A, u. Myristic acid, v. Bisandrographolide, w. Batimastat.

Fig4

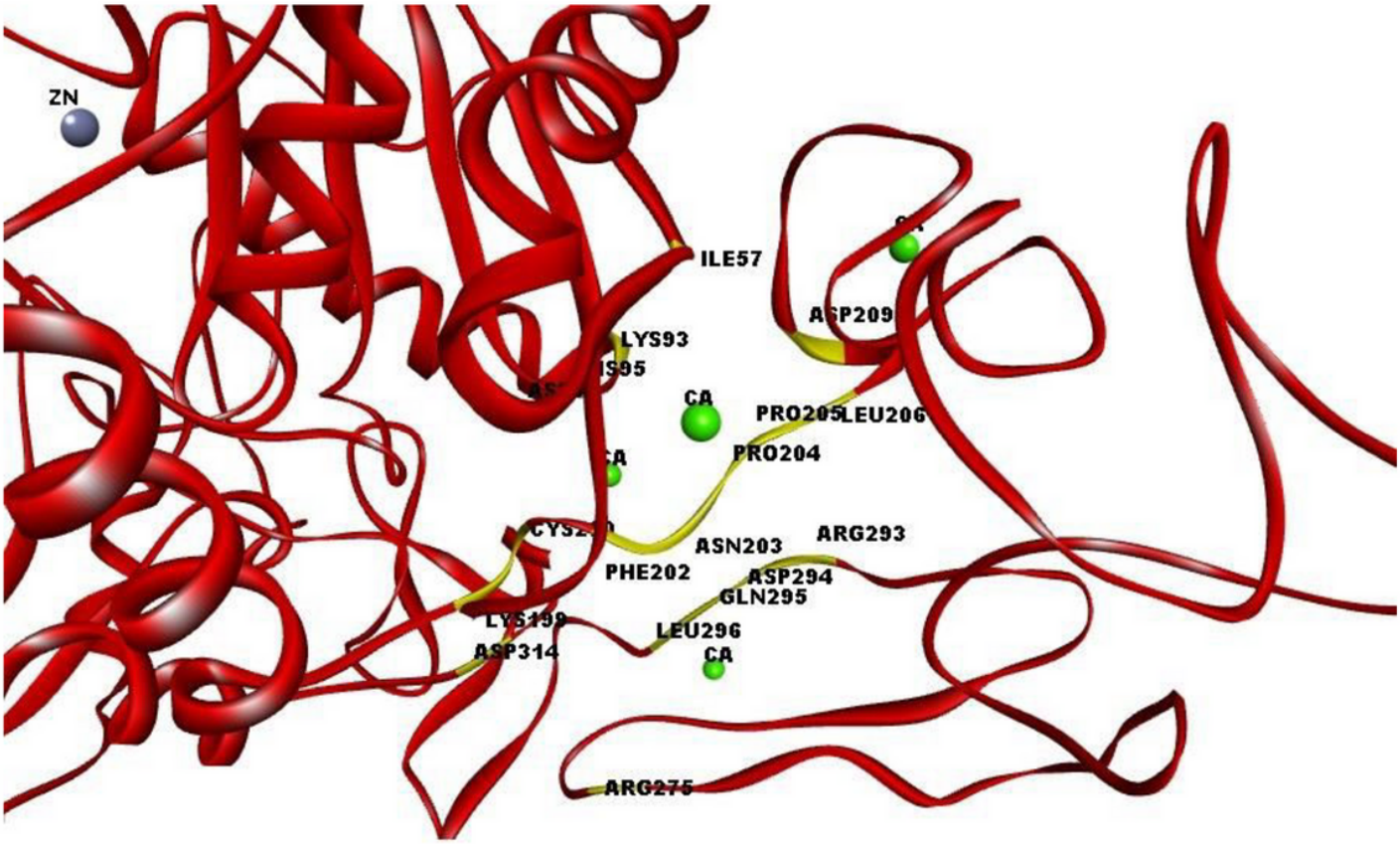

Figure 4

Catalytic calcium binding site residues interacting with the ligands

Fig5

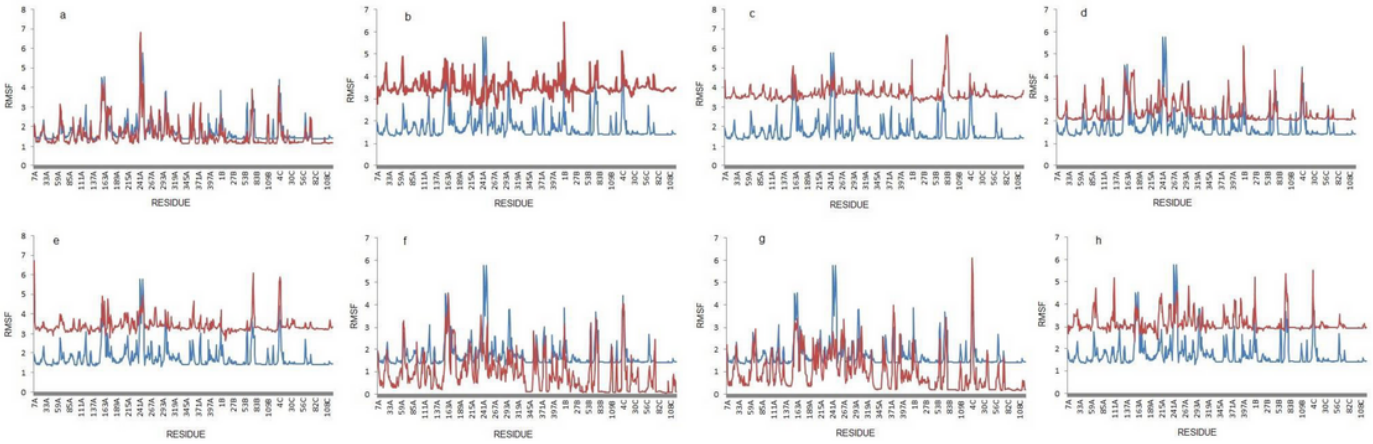

Figure 5

Molecular dynamic simulation of metalloproteinase-ligand complex. Legend: Molecular dynamic simulation of metalloproteinase (blue) with the ligands (red) a. 14-acetylandrographolide, b. 14-deoxy-11,12didehydroandrographolide, c. Andrograpanin, d. Isoandrographolide, e. 14-deoxy-11-oxoandrographolide, f. Andropanolide, g. Andrographolide, h.Batimastat.

Fig6

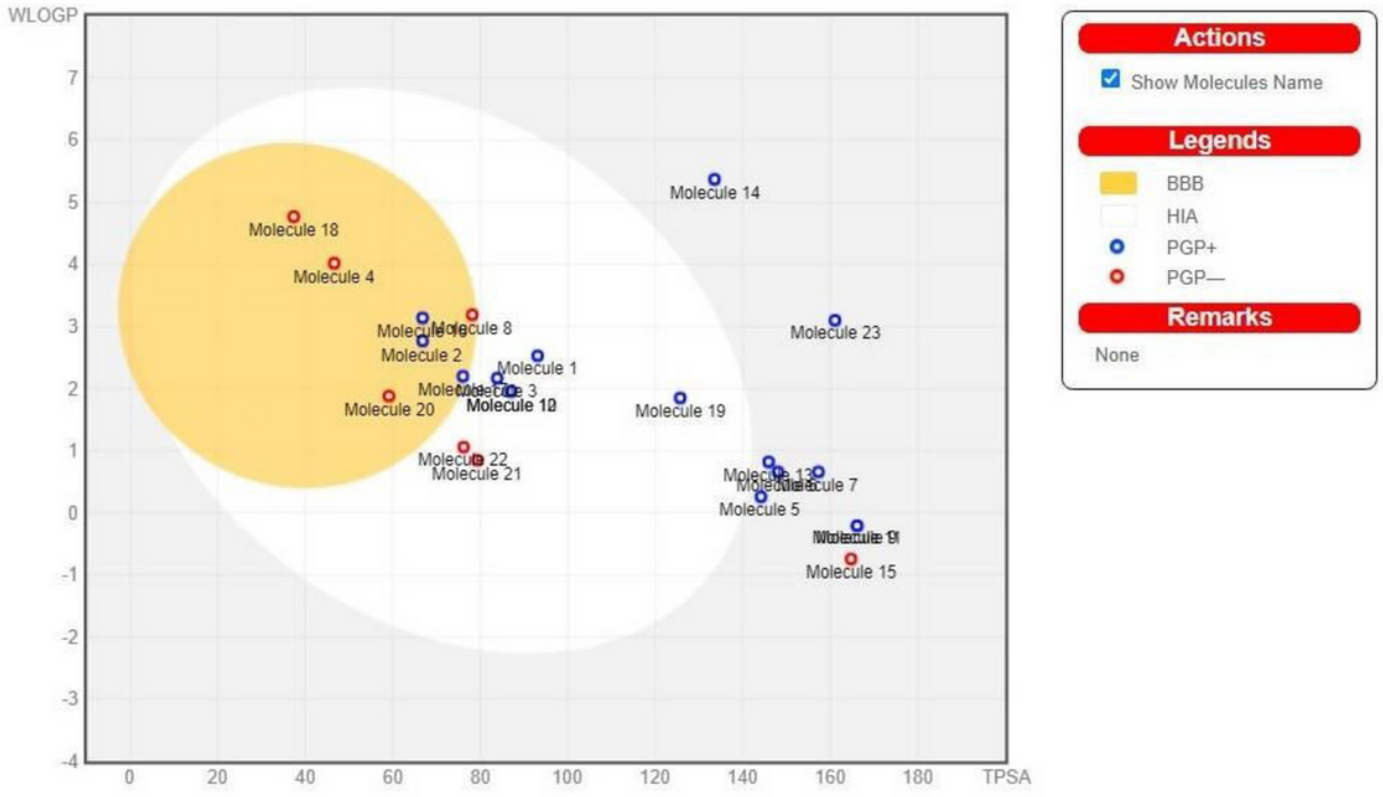

Figure 6

The BIOLED-Egg model for A.paniculata phytochemicals Legend: BOILED-Egg model representing the HIA (passive human gastrointestinal absorption), BBB (Blood brain barrier) permeation by calculating lipophilicity (WLOGP) versus polarity of phytochemicals. Molecule 1. 14-acetylandrographolide, 2. 14-deoxy-11,12didehydroandrographolide, 3. 14-deoxy-11-oxoandrographolide, 4. Andrograpanin, 5. Andrographidine A, 6. Andrographidine C, 7. Andrographidine E, 8. Andrographin, 9. Andrographiside, 10. Andrographolide, 11. Andrographoside, 12, Andropanolide, 13. Andropanoside, 14. Bisandrographolide, 15. Chlorogenic acid, 16. Deoxyandrographolide, 17. Isoandrographolide, 18. Myristic acid, 19. Neoandrographolide, 20. Paniculide A, 21. Paniculide B, 22. Paniculide

FIg7

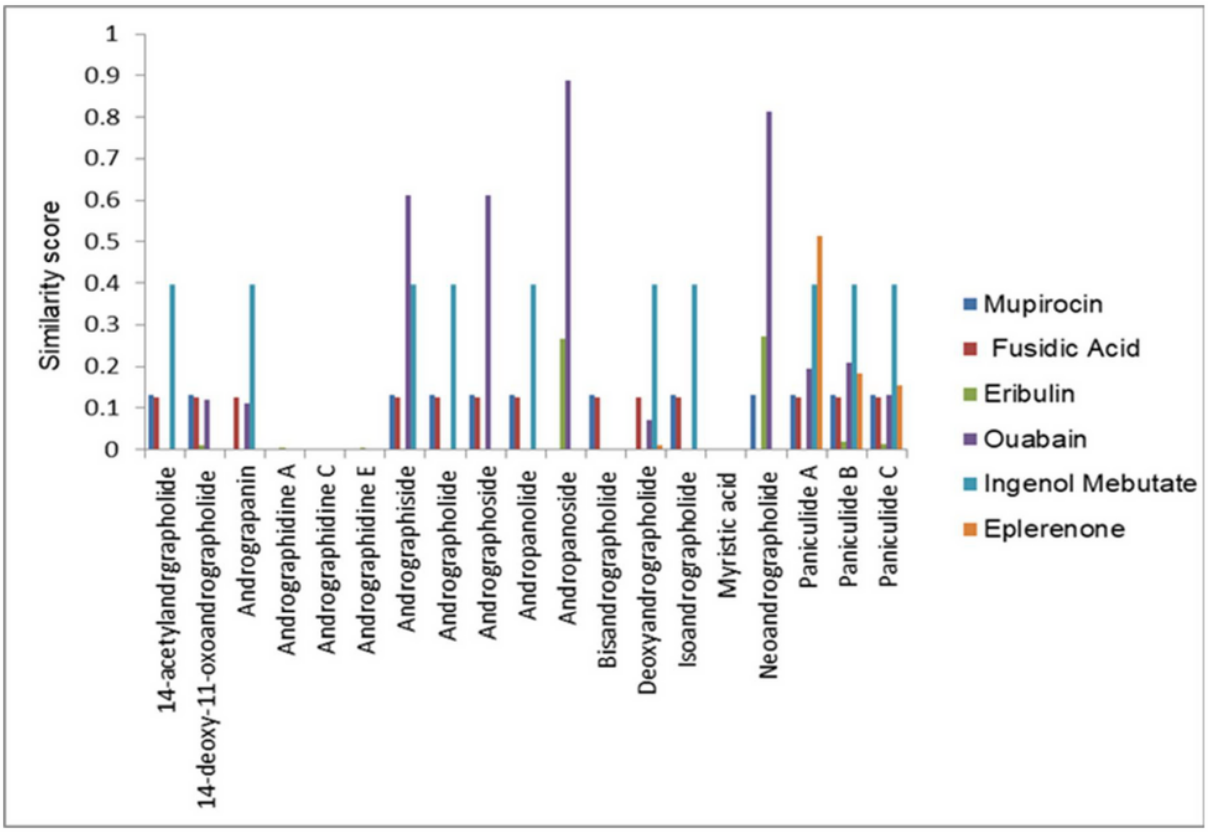

Figure 7

SwissSimilarity Results

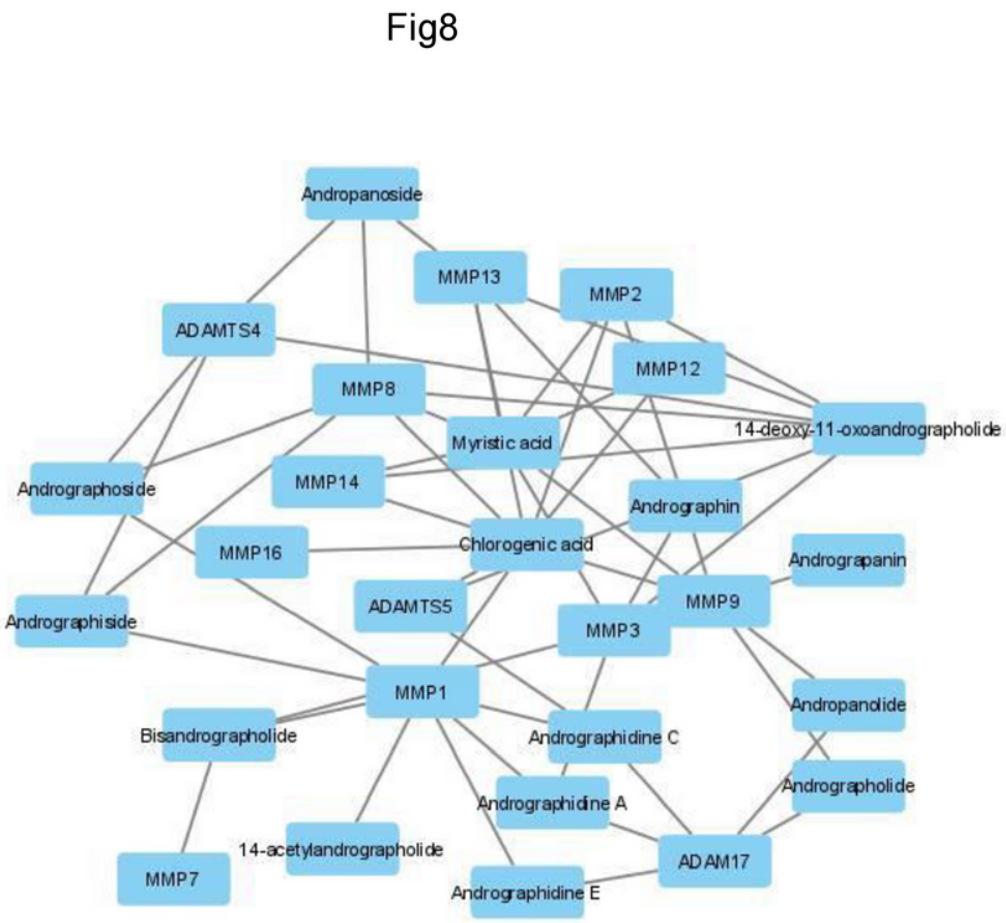

Figure 8

Phytochemical-target network

Supplementary Files

This is a list of supplementary files associated with this preprint. Click to download.

- Tables.pdf